Electronic Supplementary Information (ESI) To:

Striking ligand-disproportionative Cl/aryl scrambling in a simple Au(III) system. Solvent role, driving forces and mechanisms

*Sara Fernández-Moyano, Marconi N. Peñas-Defrutos, Camino Bartolomé, and Pablo Espinet**

IU CINQUIMA/Química Inorgánica, Facultad de Ciencias, Universidad de Valladolid, E–47071 Valladolid, Spain

E–mail: espinet@qi.uva.es

1. General information

All reactions were carried out under nitrogen atmosphere using Schlenk–tube techniques. Dichloromethane (DCM), diethyl ether (Et_2O) and hexane were obtained oxygen– and water–free from an SPS PS–MD–5 solvent purification apparatus. Toluene and chloroform were dried by the usual procedures and distilled under argon prior to be used.[1] The precursor $NBu_4[AuRf_2]$ was prepared according to the published methods.[2]

The technical measurements were carried out with equipment of the LTI services or the IU CINQUIMA (both of the University of Valladolid) unless otherwise stated.

^1H and ^{19}F NMR spectra were recorded on Bruker AV–400 and/or Varian 500/54 Premium Shielded instrument. Chemical shifts (in δ units, parts per million) were referenced to the residual solvent peaks (^1H),[3] or $CFCl_3$ (^{19}F). Coupling constants (*J*) are given in hertz (Hz). The following abbreviations are used to describe peak patterns when appropriate: s (singlet), d (doublet), t (triplet), q (quintet), m (multiplet), br (broad).

The elemental analyzes were performed by the Elemental Analysis Unit of the University of Vigo on a Carlo Erba 1108 CHN analyzer.

2. Synthesis and characterisation of the compounds, with OEt_2 as co-solvent.

Synthesis of (NBu_4)*trans*-[$AuRf_2Cl_2$] (1): A solution of Cl_2 in CCl_4 (1.3 mL, 1.03 M, 1.31 mmol) stored at 253 K was added dropwise to a solution of (NBu_4)[$AuRf_2$] (500 mg, 0.60 mmol) in dry dichloromethane (20 mL) keeping the temperature at 273 K. After 1 hour stirring at 273 K, the solvent was evaporated and the residue was recrystallized from dichloromethane-hexane, washed with hexane and vacuum dried. **1** was isolated as a white solid. **Yield:** 456 mg (84 %). Crystals valid for X-ray diffraction analysis were obtained by slow diffusion of *n*-hexane in a solution of the compound in CH_2Cl_2. The molecular structure of **1** is showed in Figure ESI5 (see X-ray section for details). **Anal. Calcd** for $C_{28}H_{36}AuCl_6F_6N$: C, 36.95; H, 3.99; N, 1.54. **Found**: C, 37.09; H, 4.16; N, 1.49.

^{19}F NMR (376.21 MHz, $CDCl_3$, 298 K): δ –97.66 (s, $4F_o$), –117.18 (s, $2F_p$).

^{1}H NMR (399.86 MHz, $CDCl_3$, 298 K): δ 3.04 (m, 8H, N*Bu*$_4^+$), 1.54 (m, 8H, N*Bu*$_4^+$), 1.34 (m, 8H, N*Bu*$_4^+$), 0.95 (t, 12H, $J_{H\text{-}H}$ = 7.3 Hz, N*Bu*$_4^+$).

Synthesis of (NBu_4)*cis*-[$AuRf_2Cl_2$] (2): A toluene solution of *trans*–isomer **1** (280 mg, 0.31 mmol) was refluxed for 6 h. After that time, the solvent was removed under reduced pressure and the residue was recrystallized from dichloromethane-hexane, washed with hexane and vacuum dried. **2** was isolated as a white solid. **Yield:** 236 mg (84 %). Crystals valid for X-ray diffraction analysis were obtained by slow diffusion of *n*-hexane in a solution of the compound in CH_2Cl_2. The molecular structure of **2** is showed in Figure ESI6 (see X-ray section for details). **Anal. Calcd** for $C_{28}H_{36}AuCl_6F_6N$: C, 36.95; H, 3.99; N, 1.54. **Found**: C, 37.24; H, 4.07; N, 1.47.

^{19}F NMR (376.21 MHz, $CDCl_3$, 298 K): δ –95.41 (s, $4F_o$), –115.35 (s, $2F_p$).

^{1}H NMR (399.86 MHz, $CDCl_3$, 298 K): δ 3.26 (m, 8H, N*Bu*$_4^+$), 1.68 (m, 8H, N*Bu*$_4^+$), 1.49 (m, 8H, N*Bu*$_4^+$), 1.04 (t, 12H, $J_{H\text{-}H}$ = 7.3 Hz, N*Bu*$_4^+$).

Halide Extraction over (NBu_4)*trans*-[$AuRf_2Cl_2$] (1). Synthesis of 3-OH_2 and 6.

1 equiv. of $AgClO_4 \cdot H_2O$[4] was added to a solution of (NBu_4)*trans*-[$AuRf_2Cl_2$] (**1**) in a mixture of diethyl ether and CH_2Cl_2 (1:1 volume), and the mixture was stirred for 1 h at room temperature shielded from the light. AgCl was filtered off and the filtrate was evaporated to dryness. The residue was extracted with diethyl ether and the insoluble NBu_4ClO_4 was filtered off. A mixture of species **3**, **4** and **5** (Scheme 1) were observed in the ^{19}F NMR spectrum (Figure 1).

[AuRf$_3$(OH$_2$)]·2OEt$_2$ (3-OH$_2$): $AgClO_4 \cdot H_2O$ (226 mg, 1.00 mmol) was added slowly to a solution of **1** (910 mg, 1.00 mmol) and the procedure above commented was followed. Then, hexane was added to the mixture of species of Figure 1 (Et_2O solution) and the solvent was evaporated slowly until the appearance of colorless crystals of **3-OH$_2$**, valid for X-ray diffraction analysis (see Figure 3 for the molecular structure). **Yield**: 206 mg (21%). **Anal. Calcd** for $C_{26}H_{22}AuCl_6F_9O_3$: C, 32.42; H, 2.30. **Found**: C, 32.57; H, 2.34.

^{19}F NMR (470.17 MHz, Et_2O, ref acetone-d_6, 298 K): δ –95.60 (q, J = 7.6 Hz, 2F$_o$), –97.21 (t, J = 7.6 Hz, 4F$_o$), –115.35 (s, 2F$_p$), –115.53 (s, 1F$_p$).

(μ-Cl)$_2$[AuRf$_2$]$_2$ (6): $AgClO_4 \cdot H_2O$ (16 mg, 0.073 mmol) was added slowly to a solution of **1** (67 mg, 0.073 mmol) and the procedure above commented was followed. Then, the Et_2O solution was evaporated until dryness and the residue was crystallized in a mixture chloroform/hexane. **6** was isolated as a white solid, washed with hexane and vacuum dried. Yield (29 mg, 62%). Crystals valid for X-ray diffraction analysis were obtained by diffusion of *n*-hexane in a solution of the compound in Et_2O (see Figure 4 for the molecular structure). **Anal. Calcd** for $C_{24}F_{12}Cl_{10}Au_2$: C, 22.79. **Found**: C, 22.63.

*Note that this compound is scarcely stable both in solid state and its solutions in non-coordinating solvents. Evolution to the homocoupling product Rf–Rf is observed.[5]

^{19}F NMR (376.47 MHz, $CDCl_3$, 298 K): δ –95.69 (s, 8F$_o$), –108.03 (s, 4F$_p$).

***cis*-[AuRf$_2$Cl(solv)] (4):** Unique species in solution when **6** was dissolved in Et_2O (Figure 2 below) or alternatively, after the procedure above commented for the halide extraction with (NBu_4)*cis*-[$AuRf_2Cl_2$] (**2**) as reagent.

^{19}F NMR (470.17 MHz, Et_2O, ref acetone-d_6, 298 K): δ –96.24 (m, 2F$_o$), –97.46 (m, 2F$_o$), –114.00 (s, 1F$_p$), –114.92 (s, 1F$_p$).

[AuRfCl$_2$(solv)] (5): Species detected in the mixture observed by ^{19}F NMR (spectrum showed Figure 1), formed as a result of the aryl scrambling.

^{19}F NMR (470.17 MHz, Et_2O, ref acetone-d_6, 298 K): δ –98.74 (br, 2F$_o$), –114.87 (br, 1F$_p$).

***cis*-[AuRf$_2$Cl(NCMe)] (7):** Unique species in solution when **6** was dissolved in NCMe.

^{19}F NMR (470.17 MHz, NCMe, ref acetone-d_6, 298 K): δ –97.11 (m, 2F$_o$), –98.47 (m, 2F$_o$), –114.81 (m, 2F$_p$).

^{19}F NMR (470.17 MHz, NCMe/toluene, ref acetone-d_6, 298 K): δ –96.57 (m, 2F$_o$), –97.76 (m, 2F$_o$), –112.61 (s, 1F$_p$), –113.11 (s, 1F$_p$).

3. Aryl Scrambling in other conditions

We have tested the initial reaction from **1** with MeCN instead of Et_2O (in the same CH_2Cl_2:co-solvent = 1:1 ratio) and neither halide abstraction nor formation of AgCl is observed. In this proportion MeCN seems to complex Ag^+ and make inefficient the Cl^- abstraction.

Note that in the solvent mixture CH_2Cl_2:Et_2O = 1:1 the silver perchlorate is only sparingly soluble, and the slow incorporation to the reaction contributes to the selective precipitation of one Cl^- per gold. Moreover, the competitive reactions (aryl rearrangement and topomerization) are fast. For these reasons, a formal kinetic treatment of the results is not possible.

A) With added MeCN

1 equiv. of $AgClO_4 \cdot H_2O$ (4.0 mg, 0.018 mmol) was added to a solution of **1** (16.2 mg, 0.018 mmol) in a mixture of diethyl ether, CH_2Cl_2 (1:1 volume) and 5 µL of acetonitrile. The mixture was stirred for 1 h at room temperature, shielded from the light and then AgCl was filtered off.

The ^{19}F NMR spectrum of the reaction aliquot is showed in Figure ESI1. Lower ratio of aryl rearrangement is observed in these conditions (≈ 40%) than in the absence of MeCN (≈ 65%, see Figure 1). Preferred coordination of MeCN is confirmed.

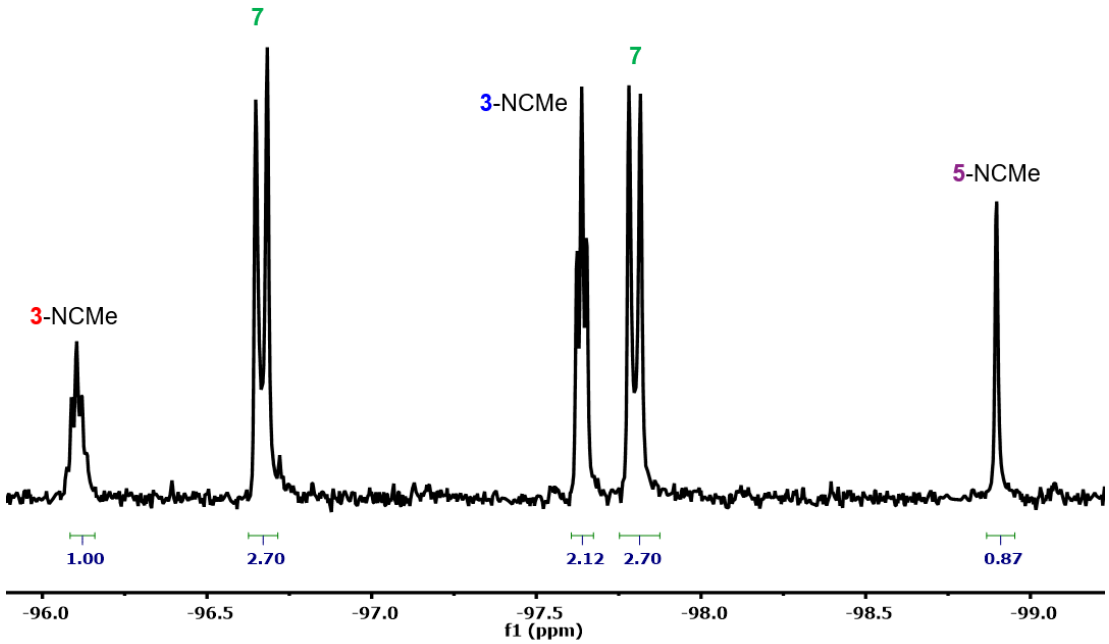

Figure ESI1. Expansion of the F_{ortho} region of the ^{19}F NMR spectrum from the reaction aliquot (in CH_2Cl_2/Et_2O, ref. acetone-d_6) with integrated signals.

B) With substoichiometric silver

0.5 equiv. of $AgClO_4 \cdot H_2O$ (2.25 mg, 0.010 mmol) was added to a solution of **1** (18.2 mg, 0.020 mmol) in CH_2Cl_2/Et_2O and the mixture was stirred for 1 h at room temperature, shielded from the light. AgCl was filtered off and the filtrate was evaporated to dryness. The residue was extracted with diethyl ether and the insoluble NBu_4ClO_4 was filtered off. The ^{19}F NMR spectrum shows the mixture of species formed (Figure ESI2). In addition to the signals of neutral **3**, **4** and **5**, the anionic complexes **1**, **2** but also $[AuRf_3Cl]^-$ and $[AuRfCl_3]^-$ can be observed, presumably formed by Cl^-/solv ligand exchanges.

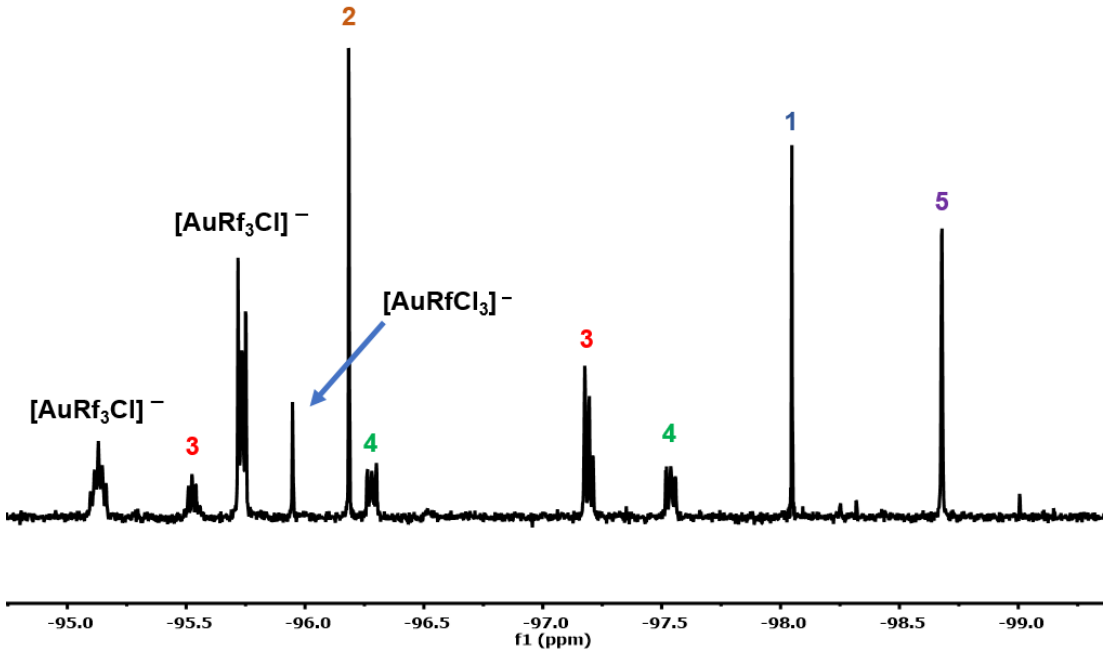

Figure ESI2. Expansion of the F_{ortho} region of the ^{19}F NMR spectrum from the reaction aliquot (in Et_2O, ref. acetone-d_6) with signal assignment.

C) With overstoichiometric silver

2 equiv. of $AgClO_4 \cdot H_2O$ (9.0 mg, 0.040 mmol) were added to a solution of **1** (18.2 mg, 0.020 mmol) in CH_2Cl_2/Et_2O and the mixture was stirred for 1 h at room temperature shielded from the light. AgCl was filtered off and the filtrate was evaporated to dryness. The residue was extracted with diethyl ether. Formation of **3**, but also the appearance of Au^0 nanoparticles were observed, probably due to the formation of scarcely stable cationic species generated after double halide abstraction.

From the Et_2O solution, crystals of $NBu_4[AuRf_4]$ (**8**) were obtained (see Figure ESI 7). Complex **8** is the result of aryl scrambling.

4. Reductive elimination from *cis*-$AuRf_2Cl$ complexes

Table ESI1 summarizes the experimental conditions (solvent, temperature…) in order to observe the formation of Rf–Rf from different *cis*-[$AuRf_2ClL$'] species with L' = μ-Cl (**6**), OEt_2 (**4**), NCMe (**7**) and Cl^- (**2**). The RE rates are **6** >> **4** > **7** >> **2**.

The homocoupling percentage was obtained by integration of the corresponding signals of the ^{19}F NMR spectra, all recorded at 293 K. Figures ESI3 and ESI4 show representative examples.

Table ESI1. Reductive elimination data from different *cis*-$AuRf_2Cl$ complexes. Solvent mixtures solv/toluene (solv = Et_2O, NCMe) are in 20:80 molar ratios.

	Solvent	**Time**	**Temperature**	**% Rf–Rf**
$(\mu\text{-}Cl)_2[AuRf_2]_2$ (**6**)	$CDCl_3$	5 h	293 K	25 % (Figure ESI3)
cis-$[AuRf_2Cl(OEt_2)]$ (**4**)	Et_2O	24 h	307 K	< 1%
cis-$[AuRf_2Cl(OEt_2)]$ (**4**)	Et_2O/Toluene	3 h	333 K	30 %
cis-$[AuRf_2Cl(NCMe)]$ (**7**)	NCMe/Toluene	3 h	333 K	< 1%
cis-$[AuRf_2Cl(NCMe)]$ (**7**)	NCMe/Toluene	1 h	353 K	5 %
(NBu_4)*cis*-$[AuRf_2Cl_2]$ (**2**)	Toluene	96 h	373 K	2 % (Figure ESI4)

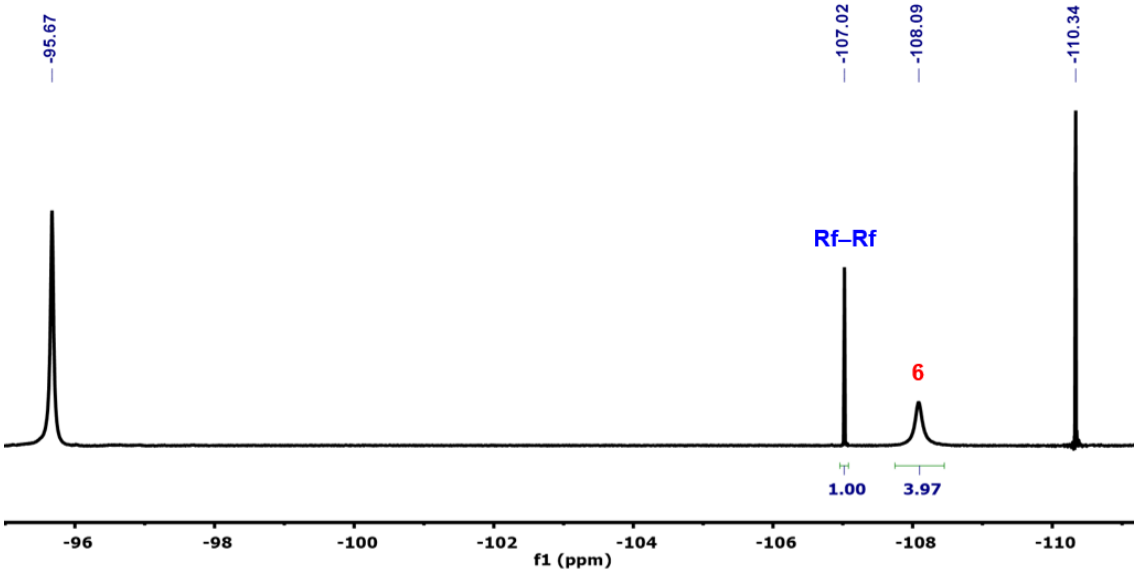

Figure ESI3. ^{19}F NMR spectrum recorded from a solution of **6** in $CDCl_3$ after 5 hours at 293 K with integrated F_{para} signals.

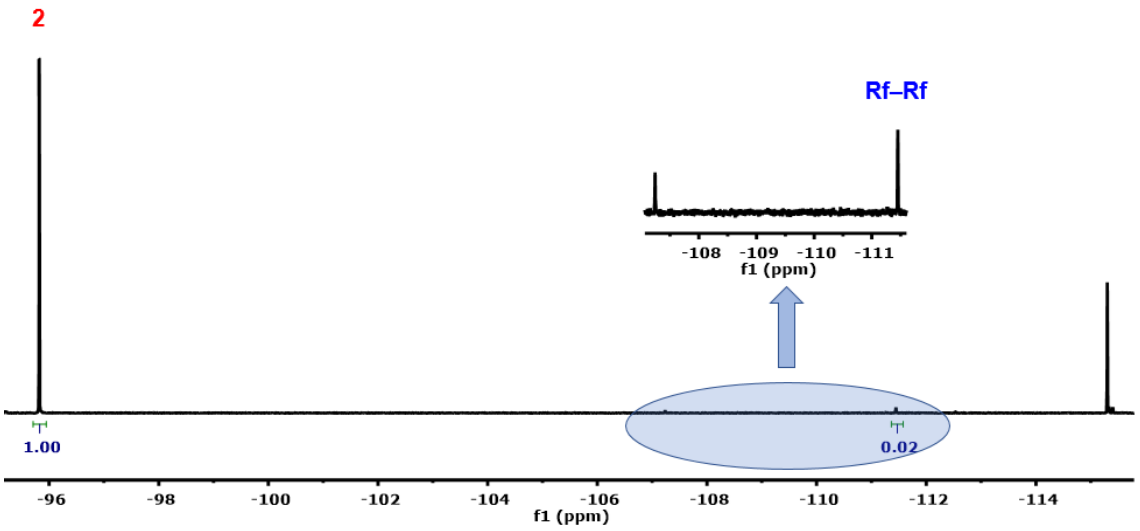

Figure ESI4. ^{19}F NMR spectrum from a solution of **2** in toluene-d_8 after 4 days at 373 K with integrated F_{ortho} signals. Expansion of the Rf–Rf signals is showed.

5. X-ray diffraction details

Refinement of the X-ray structures gives the residuals shown in Tables ESI2 and ESI3.

A crystal was attached to a glass fiber and transferred to an Agilent Supernova diffractometer with an Atlas CCD area detector. Data collection was performed with Mo-Kα radiation (λ = 0.71073 Å). Data integration, scaling and empirical absorption correction was carried out using the CrysAlisPro program package.[6] The crystal was kept at 294 K during data collection. Using Olex2,[7] the structure was solved with the ShelxT,[8] and refined with Shelx program.[9] The non-hydrogen atoms were refined anisotropically and hydrogen atoms were placed at idealized positions and refined using the riding model. CCDC 2025754-2025757 and 2043412 contains the supporting crystallographic data for this paper. These data can be obtained free of charge at www.ccdc.cam.ac.uk/conts/retrieving.html [or from the Cambridge Crystallographic Data Centre, 12, Union Road, Cambridge CB2 1EZ, UK; fax: (internat.) +44-1223/336-033; E-mail: deposit@ccdc.cam.ac.uk]. Figures 3, 4, ESI5, ESI6 and ESI7 show the molecular structures obtained.

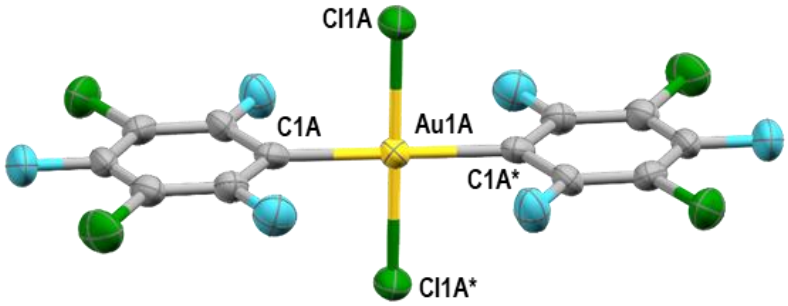

Figure ESI5. Molecular structure of **1**. NBu_4^+ is omitted for clarity. Only one of the two slightly different molecules is showed. Selected bond lengths (Å) and angles (°): Au(1A)–C(1A) = 2.046(6); Au(1A)–Cl(1A) = 2.2708(18); C(1A)–Au(1A)–Cl(1A) = 89.46(16); C(1A)–Au(1A)–Cl(1A*) = 90.54(16).

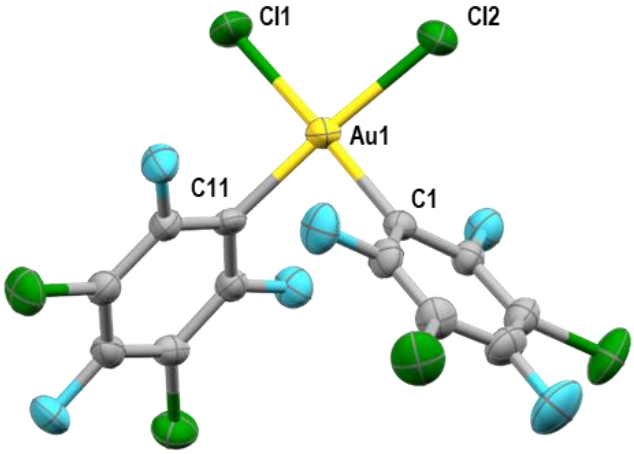

Figure ESI6. Molecular structure of **2**. NBu_4^+ is omitted for clarity. Selected bond lengths (Å) and angles (°): Au(1)–C(1) = 2.037(8); Au(1)–C(11) = 2.026(8); Au(1)–Cl(1) = 2.325(3); Au(1)–Cl(2) = 2.326(3); Cl(1)–Au(1)–Cl(2) = 92.56(11); C(1)–Au(1)–Cl(2) = 89.0(2); C(11)–Au(1)–Cl(1) = 90.9(2); C(11)–Au(1)–C(1) = 87.5(3).

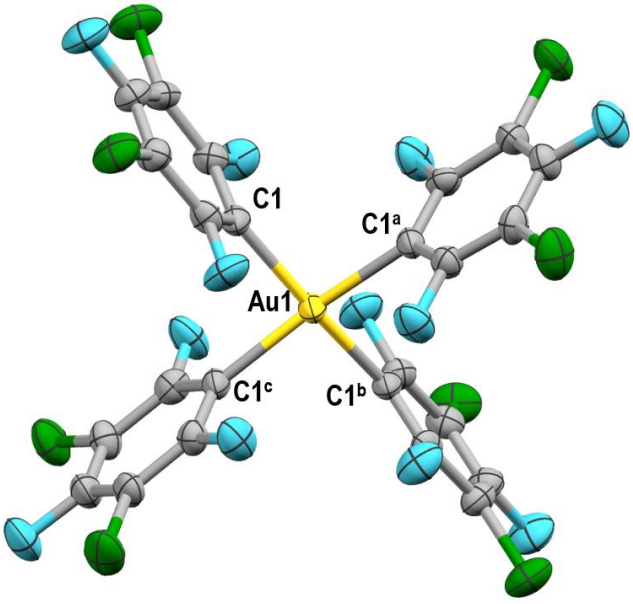

Figure ESI7. Molecular structure of $[AuRf_4]^-$ (**8**). NBu_4^+ is omitted for clarity. Selected bond lengths (Å) and angles (°): Au(1)–C(1) = 2.059(5); C(1)–Au(1)–C(1^a) = 90.46(3); C(1)–Au(1)–C(1^b) = 169.7(6).

Table ESI2. Crystal data and structure refinements for complexes **1** and **2**.

	1	**2**
Empirical formula	$C_{28}H_{36}NF_6Cl_6Au$	$C_{28}H_{36}NF_6Cl_6Au$
Formula weight	910.24	910.24
Temperature/K	294	294
Crystal system	triclinic	triclinic
Space group	P-1	P-1
a/Å	10.2702(7)	9.7193(6)
b/Å	12.5565(9)	12.2962(7)
c/Å	16.0292(11)	15.3889(9)
α/°	103.351(6)	100.005(5)
β/°	101.635(6)	97.584(5)
γ/°	110.575(6)	99.628(5)
Volume/Å^3	1789.9(2)	1760.92(19)
Z	2	2
ρ_{calc}g/cm^3	1.689	1.717
μ/mm^{-1}	4.608	4.684
F(000)	892	892.0
Crystal size/mm^3	0.4819 × 0.2124 × 0.0441	0.414 × 0.282 × 0.104
Radiation	MoKα (λ = 0.71073)	MoKα (λ = 0.71073)
2θ range for data collection/°	4.434 to 59.632	6.856 to 59.2
Index ranges	-12 ≤ h ≤ 11, -13 ≤ k ≤ 16, -21 ≤ l ≤ 16	-13 ≤ h ≤ 11, -16 ≤ k ≤ 15, -20 ≤ l ≤ 14
Reflections collected	14323	12295
Independent reflections	8424 [R_{int} = 0.0445, R_{sigma} = 0.0809]	8033 [R_{int} = 0.0347, R_{sigma} = 0.0765]
Data/restraints/parameters	8424/0/386	8033/6/303
Goodness-of-fit on F^2	1.017	1.024
Final R indexes [I>=2σ (I)]	R_1 = 0.0467, wR_2 = 0.0895	R_1 = 0.0628, wR_2 = 0.1469
Final R indexes [all data]	R_1 = 0.0905, wR_2 = 0.1130	R_1 = 0.1057, wR_2 = 0.1770
Largest diff. peak/hole / eÅ^{-3}	0.70/-1.69	2.12/-0.84

Table ESI3. Crystal data and structure refinements for complexes **3-OH$_2$** and **6** and **8**.

	3-OH$_2$	**6**	**NBu$_4$[AuRf$_4$] (8)**
Empirical formula	$C_{26}H_{22}AuCl_6F_9O_3$	$C_{24}F_{12}Cl_{10}Au_2$	$C_{40}H_{36}AuCl_8F_{12}N$
Formula weight	963.1	1264.67	1239.26
Temperature/K	294	294	294
Crystal system	monoclinic	triclinic	tetragonal
Space group	C2/c	P-1	$I4_1/a$
a/Å	17.801(4)	9.7169(8)	18.9386(7)
b/Å	12.593(3)	10.6308(6)	18.9386(7)
c/Å	17.029(3)	11.5370(7)	12.7330(9)
α/°	90	104.586(5)	90
β/°	116.43(2)	110.708(7)	90
γ/°	90	96.983(6)	90
Volume/Å^3	3418.6(13)	1049.23(13)	4567.0(5)
Z	4	1	4
ρ_{calc}g/cm^3	1.871	2.002	1.802
μ/mm^{-1}	4.849	7.689	3.770
F(000)	1856	580	2424.0
Crystal size/mm^3	0.393 × 0.185 × 0.094	0.299 × 0.133 × 0.047	0.45 × 0.049 × 0.041
Radiation	MoKα (λ = 0.71073)	MoKα (λ = 0.71073)	MoKα (λ = 0.71073)
2θ range for data collection/°	4.122 to 59.144	4.07 to 59.042	7.086 to 59.156
Index ranges	-20 ≤ h ≤ 23, -12 ≤ k ≤ 16, -22 ≤ l ≤ 17	-13 ≤ h ≤ 13, -12 ≤ k ≤ 13, -15 ≤ l ≤ 12	-17 ≤ h ≤ 26, -22 ≤ k ≤ 22, -17 ≤ l ≤ 10
Reflections collected	7035	8981	6588
Independent reflections	3940 [R_{int} = 0.0521, R_{sigma} = 0.0784]	4941 [R_{int} = 0.0372, R_{sigma} = 0.0546]	2739 [R_{int} = 0.0528, R_{sigma} = 0.0765]
Data/restraints/parameters	3940/2/209	4941/0/217	2739/0/141
Goodness-of-fit on F^2	1.015	0.967	1.079
Final R indexes [I>=2σ (I)]	R_1 = 0.0617, wR_2 = 0.1185	R_1 = 0.0340, wR_2 = 0.0619	R_1 = 0.0535, wR_2 = 0.0885
Final R indexes [all data]	R_1 = 0.1104, wR_2 = 0.1420	R_1 = 0.0518, wR_2 = 0.0689	R_1 = 0.0927, wR_2 = 0.1013
Largest diff. peak/hole / eÅ^{-3}	1.60/-1.73	1.00/-0.74	0.90/-0.88

5. Computational Section

Density functional theory (DFT) calculations reported in this work were carried out using the dispersion corrected hybrid functional ωB97X-D developed by Head-Gordon and Chai,[10] and the Gaussian09 software.[11] The choice of this level of theory is based on the satisfactory results obtained in previous theoretical studies on previous mechanistic studies with Au derivatives.[12] C and H atoms were described using the double-ζ basis set 6-31G(d,p), whereas the same basis set plus diffuse functions was employed to describe the more electronegative O, Cl and F atoms. Au was described using the effective core potential LANL2DZ[13] including f-polarization functions (exponent: 1.050).[14]

Geometry optimizations in vacuum were performed without imposing any constraint and the nature of all the stationary points was further verified through vibrational frequency analysis. The effect of the solvent employed in experiments (diethyl ether: ε = 4.2400) was introduced through single-point calculations at the optimized geometries in vacuum using the SMD solvation model.[15]

Figure ESI8 shows the optimized structure of the proposed dimeric intermediate ***I2***. Table ESI4 collects all the energy data that support the discussion made in the text about the thermodynamics of the reaction. The Cartesian coordinates of all the computed structures are collected below.

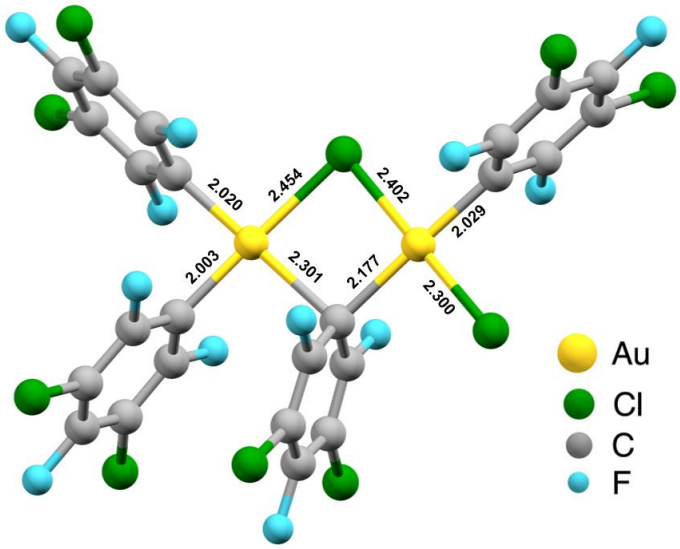

Figure ESI8. Optimized geometry of ***I2***. Selected bond lengths (Å).

Table ESI4. DFT energy data (Hartree).

	E_{gas}	G_{gas}	E_{SMD}	G_{solv}
trans-[$AuRf_2Cl(OEt_2)$] (***I1***)	-3725.92569	-3725.754923	-3725.951483	-3725.780716
cis-[$AuRf_2Cl(OEt_2)$] (**4**)	-3725.956387	-3725.783820	-3725.980795	-3725.808228
[$AuRf_3(OEt_2)$] (**3**)	-4714.096725	-4713.889343	-4714.122884	-4713.915503
trans-[$AuRfCl_2(OEt_2)$] (**5**)	-2737.802507	-2737.667990	-2737.824092	-2737.689574
cis-[$AuRfCl_2(OEt_2)$]	-2737.786057	-2737.648061	-2737.810890	-2737.672894
I2	-6984.65284	-6984.55083	-6984.68607	-6984.584063
OEt_2	-233.603314	-233.495374	-233.60935	-233.5014103

Cartesian coordinates of all the calculated species

***trans*-[AuRf$_2$Cl(OEt$_2$)] (*I1*)**

79	0.02108700	0.03204500	-0.15752300	1	-0.25897500	2.66041400	0.98968600
17	5.03531900	-2.71642000	-0.50298300	6	-0.37060800	-1.12024600	2.68000300
17	5.11646400	2.66567500	0.07714500	1	-1.43594000	-1.30184400	2.49999600
9	2.13665200	-2.31500900	-0.48762000	1	-0.21572000	-0.94161300	3.74839100
9	2.20502400	2.35538000	0.01772800	6	0.48791700	-2.26326700	2.20004300
9	6.22779200	-0.04484300	-0.19345700	1	0.24092700	-3.15231400	2.78618800
6	2.84033100	1.17557300	-0.07862400	1	0.30279000	-2.50339500	1.15115500
6	4.19671300	-1.21869700	-0.33369600	1	1.54859200	-2.04043300	2.33593500
6	4.23304400	1.19155900	-0.07329700	6	-2.05591000	0.00207900	-0.18073400
6	2.09110200	0.01635600	-0.18065600	6	-2.75865500	-1.18411700	-0.05919700
6	4.89732100	-0.02426900	-0.19876300	6	-2.81709200	1.14399900	-0.36688200
6	2.80516400	-1.16093400	-0.33295400	6	-4.14856500	-1.26375900	-0.08848000
8	0.00063400	0.11659600	2.01554900	6	-4.20932100	1.14117600	-0.40602600
17	0.03786600	-0.03210900	-2.43554800	6	-4.86041800	-0.08118600	-0.26595500
6	-0.69081600	1.25880500	2.58766700	9	-2.19199700	2.32541900	-0.50211600
1	-0.54970300	1.18022300	3.66990600	9	-2.07165100	-2.32923400	0.11170800
1	-1.75827800	1.16156800	2.36015700	9	-6.18964300	-0.11903000	-0.29627900
6	-0.10845600	2.54796200	2.06561500	17	-5.10833100	2.59676300	-0.62144600
1	-0.61788200	3.38199300	2.55565500	17	-4.97083300	-2.76934500	0.08764400
1	0.95885700	2.61312200	2.28302300				

***cis*-[AuRf$_2$Cl(OEt$_2$)] (4)**

79	-0.20213500	1.32022100	0.03031700	1	-2.53821900	3.70291800	2.88176900
17	-1.64009600	-3.37174900	-2.85737300	1	-3.02538700	2.11269500	2.26404900
17	-3.76436200	-2.61336500	2.06210700	1	-1.30276500	2.54004300	2.40418600
9	-0.28547400	-0.84983400	-2.26764300	6	-2.21477800	3.05741300	-1.56383800
9	-2.13793800	-0.18815400	1.99893600	1	-1.45708600	3.83955400	-1.69123300
9	-3.29727300	-3.97342400	-0.50306600	1	-3.20939400	3.51336000	-1.60976400
6	-2.01627000	-0.90119400	0.87393500	6	-2.07886200	1.97511000	-2.61094500
6	-1.78859800	-2.42730700	-1.42387700	1	-2.32248600	2.40203500	-3.58732800
6	-2.74117700	-2.08658300	0.77943300	1	-1.05996900	1.58360700	-2.67348500
6	-1.18906200	-0.43645000	-0.13726000	1	-2.76735100	1.14927100	-2.41370500
6	-2.61534900	-2.83908500	-0.38351600	6	1.46461100	0.24654800	0.20530300
6	-1.08842800	-1.23414800	-1.26743600	6	2.37504000	0.19733900	-0.83936700
17	0.99296900	3.35474200	0.20563400	6	1.77240600	-0.43313500	1.37176600
8	-2.07675700	2.50745800	-0.23255000	6	3.57153700	-0.50783500	-0.74046000
6	-2.33953500	3.51914500	0.77340800	6	2.95601500	-1.15121900	1.51955600
1	-3.33482500	3.91919300	0.55213200	6	3.84509300	-1.17560500	0.44941900
1	-1.59403700	4.31239500	0.65973500	9	0.91094800	-0.40399100	2.39194400
6	-2.29868500	2.91945500	2.15784400	9	2.10705600	0.83920300	-1.97567600

9	4.98146000	-1.85466500	0.56619100	17	4.68599200	-0.55315800	-2.05230100
17	3.31382000	-1.98641600	2.98305500				

[AuRf$_3$(OEt$_2$)] (3)

79	-0.00775500	-0.70278200	-0.01380800	1	-0.59240900	-2.00475100	2.50308400
17	-4.94322100	0.39302700	2.70456600	1	-1.91305700	-2.98680600	1.82355600
17	-5.17794600	-1.72949700	-2.26985500	6	2.06643100	-0.64830100	-0.08312700
9	-2.05573700	0.25831200	2.23571200	6	2.83891800	-1.04846300	0.99459500
9	-2.26004400	-1.58091300	-2.08136200	6	2.76503700	-0.19807600	-1.19182100
9	-6.21060200	-0.67239200	0.27281800	6	4.23104000	-1.03491700	0.99626800
6	-2.85990100	-1.12420000	-0.97079400	6	4.15537700	-0.15589200	-1.26347400
6	-4.14769300	-0.18907200	1.28936400	6	4.87535600	-0.58081900	-0.15075500
6	-4.25225300	-1.14214900	-0.93801300	9	2.07526100	0.21678200	-2.26784700
6	-2.07573400	-0.66813200	0.07571000	9	2.22109700	-1.49171900	2.10563000
6	-4.88180700	-0.66724500	0.20806200	9	6.20461800	-0.55598600	-0.18517500
6	-2.75915400	-0.19952700	1.18625200	17	4.97002700	0.40231200	-2.67674100
8	0.00169500	-2.93348300	-0.05061700	17	5.13850000	-1.55880500	2.36624300
6	0.87425600	-3.54256100	-1.02965600	6	-0.02705300	1.28839000	-0.01607600
1	0.70022400	-4.62209100	-0.97407400	6	0.45116200	2.01118700	1.06569700
1	1.91244100	-3.33900000	-0.74128100	6	-0.51387300	1.99766400	-1.10309400
6	0.56414600	-3.02746500	-2.41546500	6	0.45118000	3.40335500	1.08664300
1	1.22434200	-3.52743900	-3.12935200	6	-0.53421600	3.38964000	-1.13230600
1	-0.47136200	-3.23707500	-2.68681600	6	-0.04690100	4.07646800	-0.02462100
1	0.73732600	-1.95183700	-2.50561600	9	-0.05648500	5.40543700	-0.02849900
6	0.05618200	-3.62974900	1.21691000	9	0.93352300	1.36081100	2.12661000
1	1.08834400	-3.60536600	1.58258500	9	-0.98243700	1.33358300	-2.16135700
1	-0.22285600	-4.66810100	1.00854600	17	1.05175900	4.27146600	2.44735500
6	-0.89458000	-3.01597500	2.21720600	17	-1.14581300	4.24078900	-2.49872700
1	-0.88840600	-3.62803400	3.12302700				

***trans*-[AuRfCl$_2$(OEt$_2$)] (5)**

79	-1.09953100	-0.00000500	0.04356500	1	-3.90056400	-3.30118200	-0.01637600
17	-1.14874300	-0.00131200	-2.28548700	1	-2.29354400	-2.58116900	-0.09053100
8	-3.31224900	0.00002800	0.08260800	1	-3.31877900	-2.30543600	1.33660700
6	-3.94136700	1.20227200	-0.41115700	6	0.88605000	-0.00009400	0.01487700
1	-5.00421700	1.12181400	-0.15920300	6	1.59060200	-1.19045700	0.00014600
1	-3.83096500	1.23036900	-1.50147600	6	1.59048400	1.19035500	-0.00035600
6	-3.32020900	2.41385100	0.24854200	6	2.98225600	-1.21582500	-0.02948100
1	-3.90007600	3.30134300	-0.01838300	6	2.98212300	1.21589500	-0.02991900
1	-3.32028100	2.30613400	1.33585700	6	3.65991900	0.00006100	-0.04393500
1	-2.29309600	2.58095800	-0.09002000	9	0.92357500	2.34620000	0.01245300
6	-3.94190600	-1.20229700	-0.41016300	9	0.92383200	-2.34636300	0.01343100
1	-3.83248500	-1.23084600	-1.50058400	9	4.98878600	0.00013000	-0.07242500
1	-5.00451500	-1.12165000	-0.15726600	17	3.84340200	2.70690200	-0.04881300
6	-3.32015700	-2.41368300	0.24933700	17	3.84369800	-2.70675400	-0.04789500

17	-1.03677200	0.00114500	2.36163000

***cis*-[AuRfCl$_2$(OEt$_2$)]**

79	-1.30369100	-0.08121900	-0.39732000	6	-2.34019300	1.46431800	2.06982400
17	3.72079400	-2.61710300	0.33759900	1	-2.23646900	1.57623300	3.15370700
17	3.58946300	2.78202500	-0.01848800	1	-3.38768600	1.27668400	1.81581300
9	0.84141000	-2.35908200	-0.10587000	6	-1.80196500	2.67580000	1.35165400
9	0.72557700	2.32770300	-0.41290300	1	-2.35037500	3.55398600	1.70294200
9	4.79148100	0.12246400	0.33972000	1	-0.74088300	2.82679900	1.55687700
6	1.39519300	1.18706700	-0.21064000	1	-1.95432200	2.60817200	0.27059600
6	2.83194800	-1.15503400	0.13538300	6	-2.06925300	-0.87550300	2.47605500
6	2.77283600	1.26490100	-0.02348600	1	-3.11669500	-1.03348500	2.19955600
6	0.70383200	-0.01282600	-0.20007400	1	-2.00778800	-0.58913100	3.53072600
6	3.47620500	0.07790700	0.15439300	6	-1.22699400	-2.09617200	2.20182200
6	1.45282700	-1.17041800	-0.05744100	1	-1.55383400	-2.89927700	2.86753500
17	-3.66861900	-0.20985100	-0.57665900	1	-1.34609900	-2.45371800	1.17562100
8	-1.57711300	0.27104600	1.72954400	1	-0.16938100	-1.90025700	2.39300700
17	-0.93109900	-0.40789800	-2.61821400				

I2

79	-0.82793900	0.52593800	-0.21100600	6	-1.58048100	3.22566300	0.73688400
17	-5.27356200	-2.45667800	-2.01726500	6	-2.50125000	2.72078200	-1.39434500
17	-5.21385900	-0.76689500	3.12441700	6	-2.15876000	4.49192100	0.71800600
17	-1.81243400	-3.55266800	2.88280900	6	-3.10138500	3.97516100	-1.46383500
17	-1.45135200	-4.24885600	-2.47100200	6	-2.91880300	4.84710700	-0.39370300
9	0.30946700	-1.90067300	-2.29179800	9	-0.84522200	2.87383100	1.79356000
9	-2.73091400	-1.00296600	-2.14711200	9	-2.67318800	1.87528200	-2.41286500
9	-6.24231100	-2.14518200	0.74083700	9	-3.48134200	6.04826200	-0.43499200
9	-2.67772400	0.46401500	2.31016800	17	-1.94310000	5.58957200	2.02529200
9	0.06624900	-1.35472600	2.35698000	17	-4.04258600	4.43773100	-2.82864200
9	-2.33688100	-4.75898900	0.26976800	17	1.42319200	1.43389800	-0.57302400
6	0.20326400	-1.51824300	0.02013800	79	2.23916800	-0.74870800	0.01190800
6	-2.65102700	-0.25270300	0.07729200	6	4.15391500	-0.07750200	0.00616600
6	-0.16983600	-2.27162600	-1.11037000	6	4.91019700	-0.08781000	-1.15222100
6	-3.27100800	-0.19876700	1.31633600	6	4.74125300	0.40375100	1.16255000
6	-5.08831400	-1.52847000	0.52452400	6	6.22293800	0.37488700	-1.18570500
6	-4.51032800	-1.59378900	-0.74047200	6	6.04982700	0.87828900	1.18777600
6	-3.29671800	-0.93977800	-0.93957900	6	6.77545500	0.85365500	-0.00049500
6	-4.48375400	-0.83308500	1.56920100	9	4.36288800	-0.55121500	-2.28131000
6	-1.01228500	-3.37128300	-1.06237700	9	4.02952800	0.42083100	2.29447800
6	-0.29198200	-1.99691500	1.25096200	9	8.02647400	1.30187900	-0.00430700
6	-1.50532800	-3.73927400	0.19210700	17	7.14102500	0.35897200	-2.64308600
6	-1.15924800	-3.06819600	1.36916300	17	6.75470800	1.47976300	2.63968900
6	-1.73637400	2.32760300	-0.30868200	17	3.03737600	-2.83734500	0.5497630

6. NMR spectra

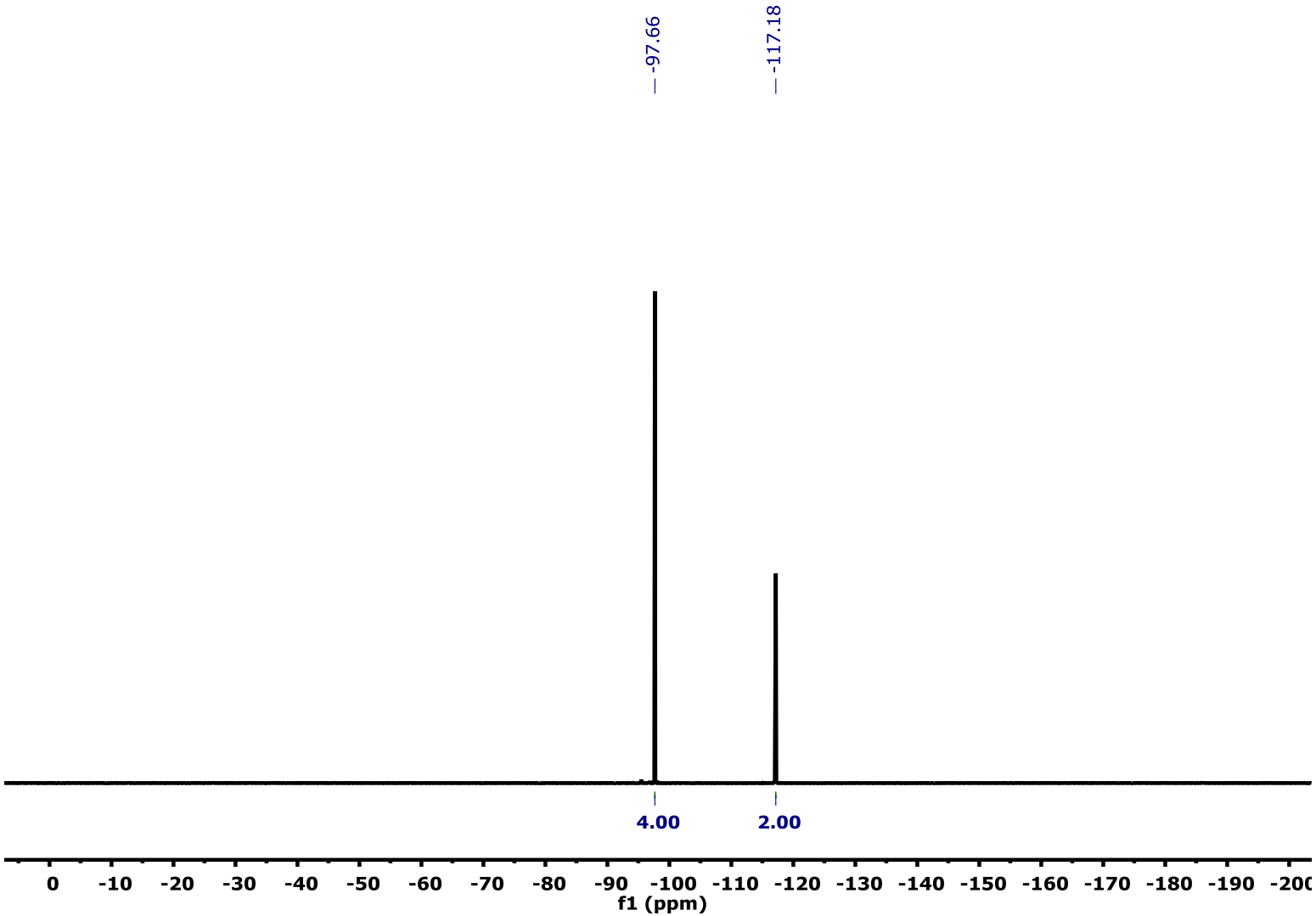

Figure ESI9. ^{19}F NMR (376 MHz, $CDCl_3$, 298 K) of (NBu_4)*trans*-$[AuRf_2Cl_2]$ (**1**).

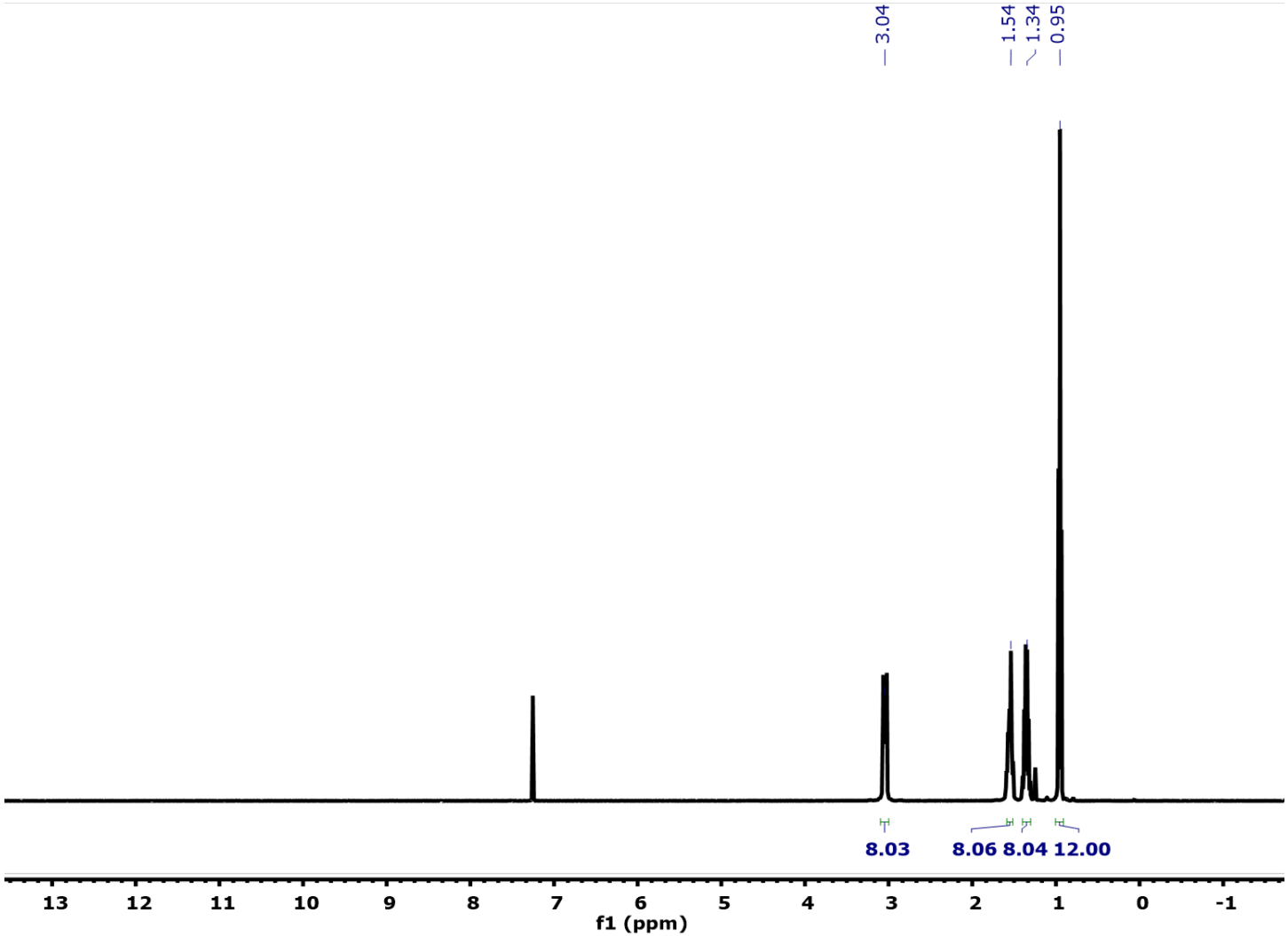

Figure ESI10. ^{1}H NMR (400 MHz, $CDCl_3$, 298 K) of (NBu_4)*trans*-$[AuRf_2Cl_2]$ (**1**).

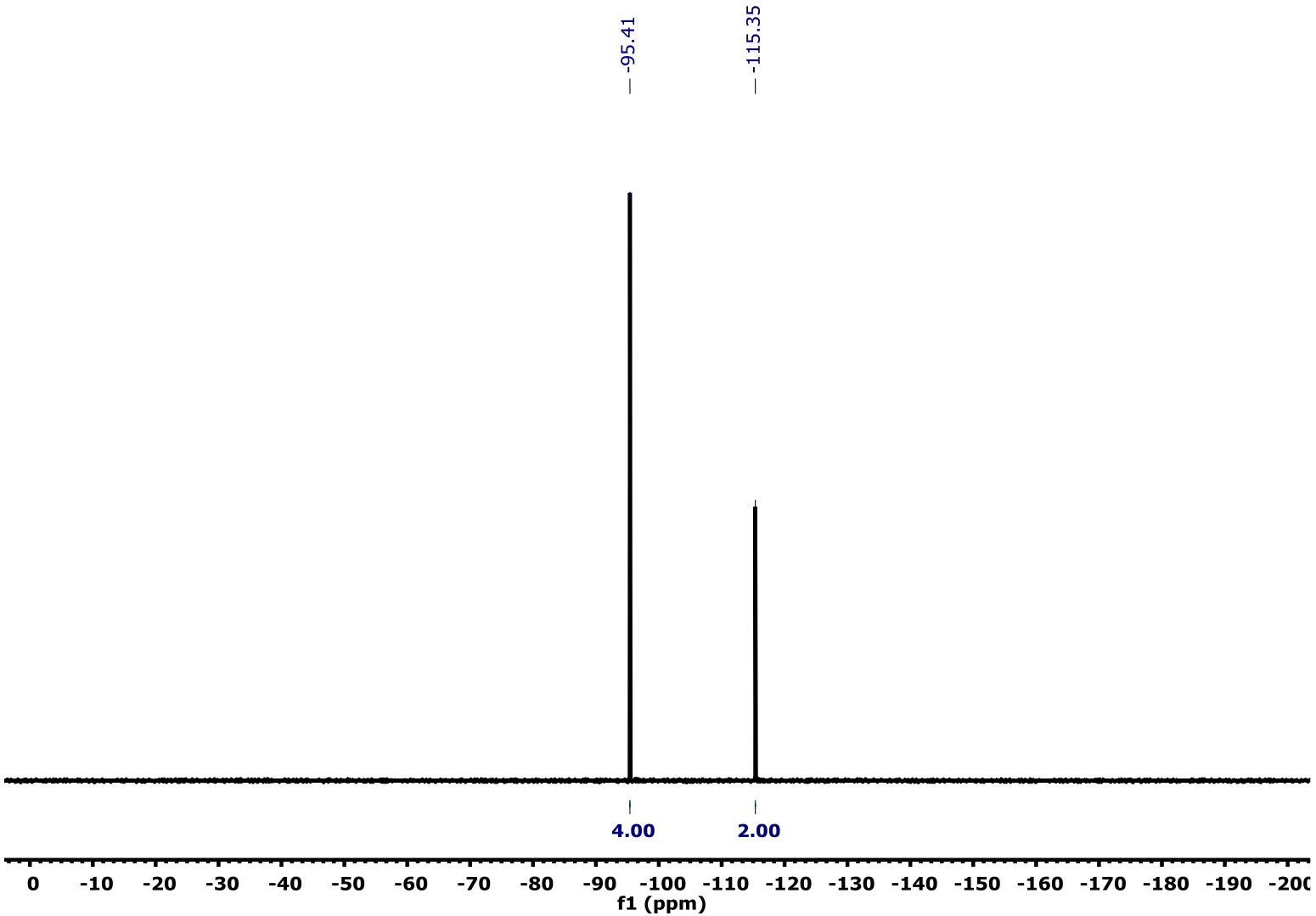

Figure ESI11. ^{19}F NMR (376 MHz, $CDCl_3$, 298 K) of (NBu_4)*cis*-$[AuRf_2Cl_2]$ (**2**).

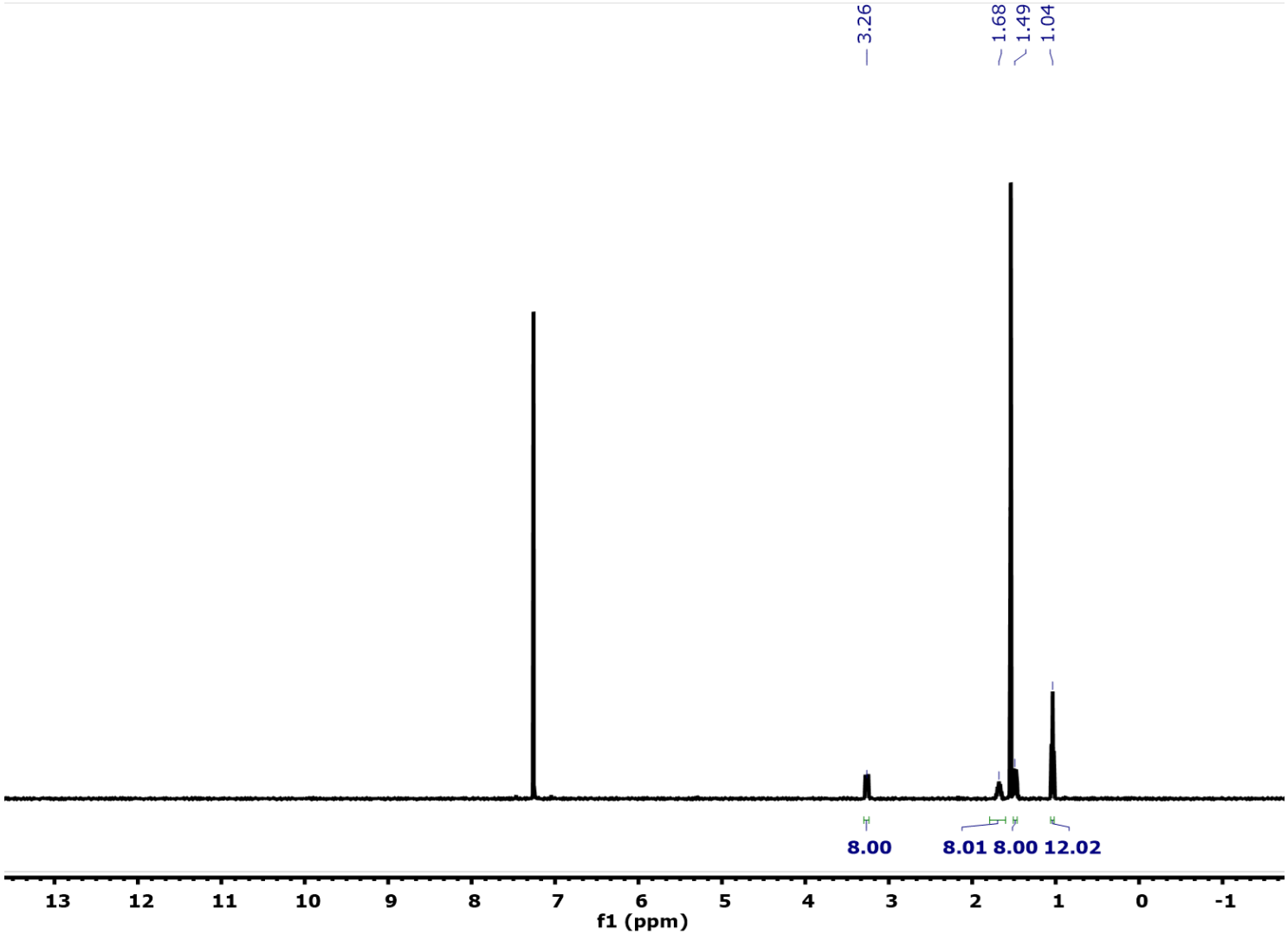

Figure ESI12. ^{1}H NMR (400 MHz, $CDCl_3$, 298 K) of (NBu_4)*cis*-[$AuRf_2Cl_2$] (**2**).

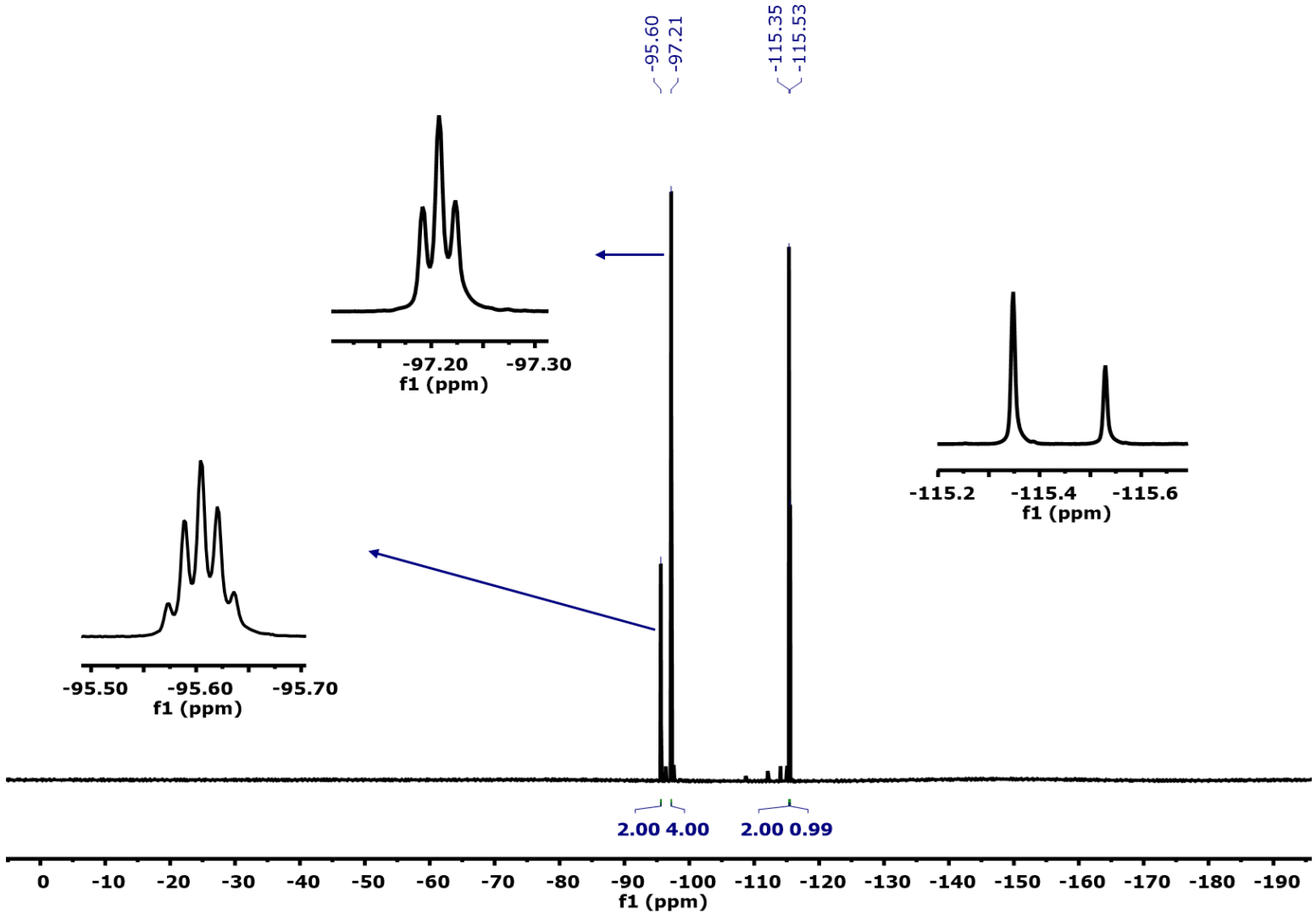

Figure ESI13. ^{19}F NMR (376 MHz, Et_2O ref. acetone-d_6, 298 K) of [$AuRf_3$(solv)] (**3**).

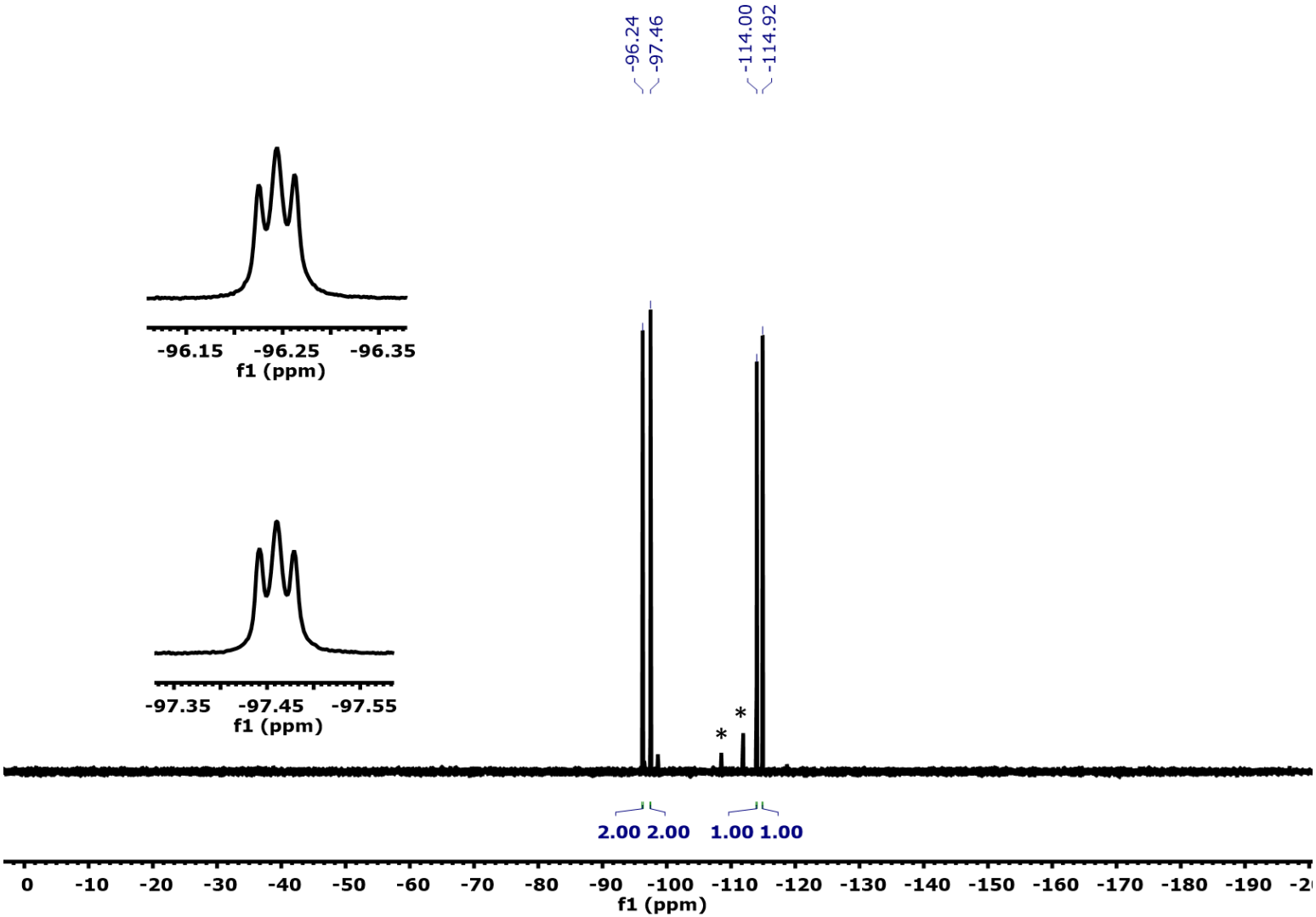

Figure ESI14. ^{19}F NMR (470 MHz, Et_2O ref. acetone-d_6, 298 K) of *cis*-[$AuRf_2Cl$(solv)] (**4**). Asterisks (*) denote signals of Rf–Rf.

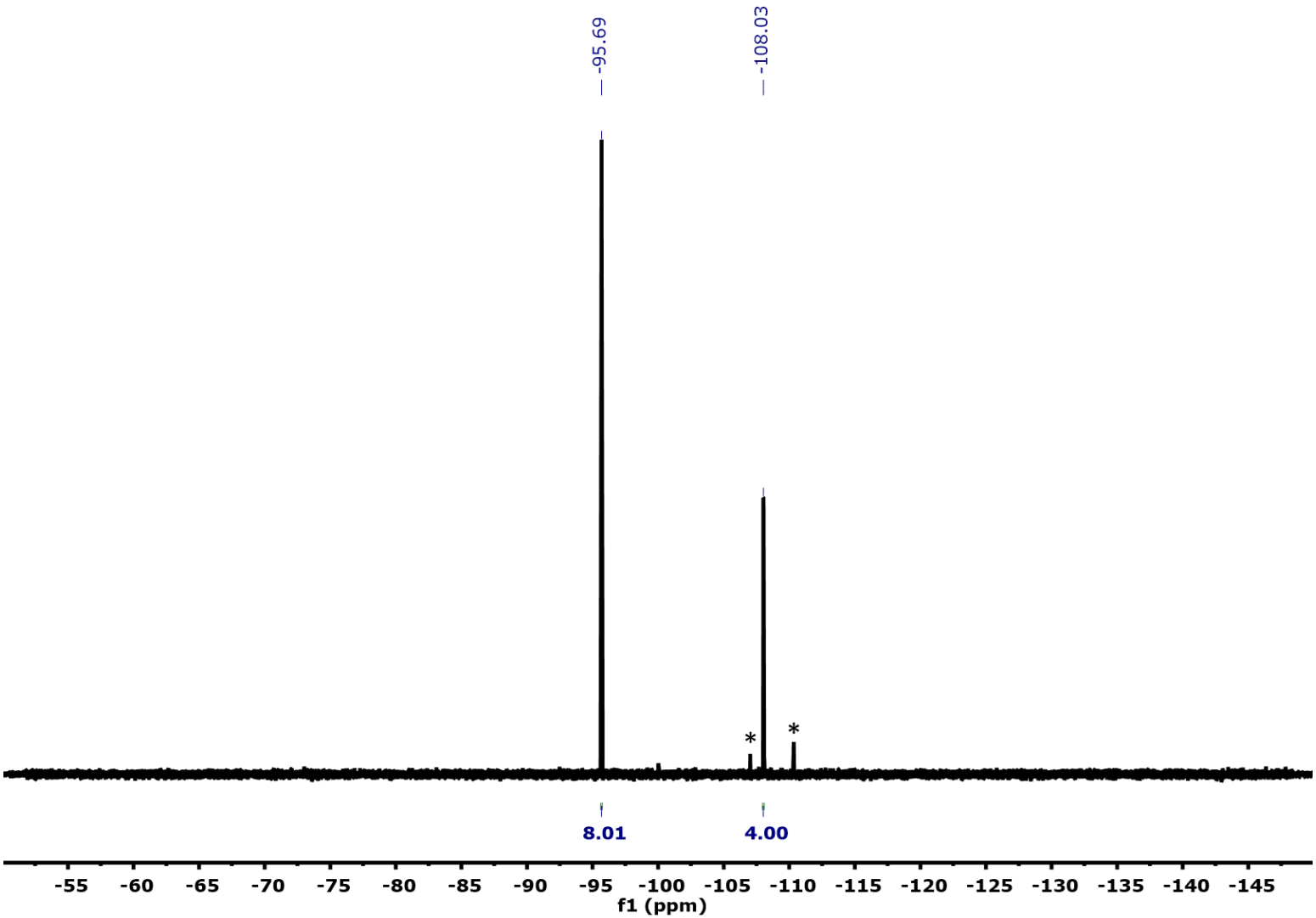

Figure ESI15. ^{19}F NMR (470 MHz, $CDCl_3$, 298 K) of $(\mu\text{-}Cl)_2[AuRf_2]_2$ (**6**). Asterisks (*) denote signals of Rf–Rf.

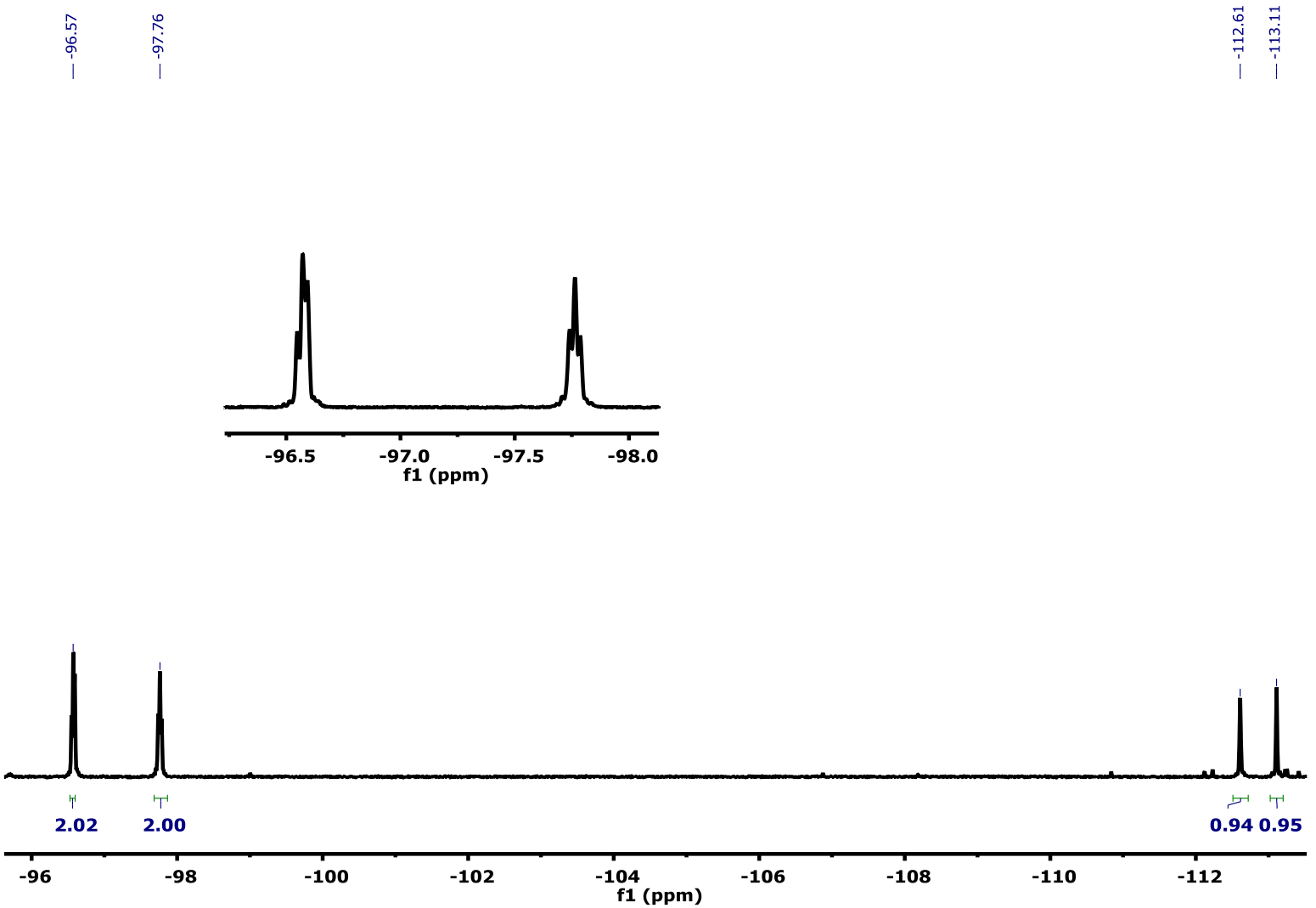

Figure ESI16. ^{19}F NMR (470 MHz, NCMe/toluene ref. acetone-d_6, 298 K) of *cis*-[AuRf$_2$Cl(NCMe)] (**7**).

7. References

1 D. B. G. Williams and M. Lawton, *J. Org. Chem.*, 2010, **75**, 8351–8354.

2 E. J. Fernández, A. Laguna, J. M. López-de-Luzuriaga, M. Monge, M. Montiel, M. E. Olmos, J. Pérez, R. C. Puelles and J. C. Sáenz, *Dalton Trans.*, 2005, 1162−1164.

3 G. R. Fulmer, A. J. M. Miller, N. H. Sherden, H. E. Gottlieb, A. Nudelman, B. M. Stoltz, J. E. Bercaw and K. G. Goldberg, *Organometallics*, 2010, **29**, 2176−2179.

4 *Caution!* Some perchlorate salts are hazardous (explosive). See: W. C. Wolsey, *J. Chem. Educ.*, 1973, **50**, A335–A337.

5 J. A. Casares, P. Espinet, J. M Martín-Alvarez, J. M. Martínez-Ilarduya and G. Salas, *Eur. J. Inorg. Chem.*, 2005, 3825–3831.

6 CrysAlisPro Software system, version 1.171.33.51, 2009, Oxford Diffraction Ltd, Oxford, UK.

7 O. V. Dolomanov, L. J. Bourhis, R. J. Gildea, J. A. K. Howard and H. Puschmann, *J. Appl. Cryst.*, 2009, **42**, 339–341.

8 G. M. Sheldrick, *Acta Cryst.*, 2015, **A71**, 3–8.

9 G. M. Sheldrick, *Acta Cryst.*, 2015, **C71**, 3–8.

10 J.-D. Chai and M. Head-Gordon, *Phys. Chem. Chem. Phys.*, 2008, **10**, 6615–6620.

11 Gaussian 09, Revision **E.01**, M. J. Frisch, G. W. Trucks, H. B. Schlegel, G. E. Scuseria, M. A. Robb, J. R. Cheeseman, G. Scalmani, V. Barone, G. A. Petersson, H. Nakatsuji, X. Li, M. Caricato, A. V. Marenich, J. Bloino, B. G. Janesko, R. Gomperts, B. Mennucci, H. P. Hratchian, J. V. Ortiz, A. F. Izmaylov, J. L. Sonnenberg, D. Williams-Young, F. Ding, F. Lipparini, F. Egidi, J. Goings, B. Peng, A. Petrone, T. Henderson, D. Ranasinghe, V. G. Zakrzewski, J. Gao, N. Rega, G. Zheng, W. Liang, M. Hada, M. Ehara, K. Toyota, R. Fukuda, J. Hasegawa, M. Ishida, T. Nakajima, Y. Honda, O. Kitao, H. Nakai, T. Vreven, K. Throssell, J. A., Jr. Montgomery, J. E. Peralta, F. Ogliaro, M. J. Bearpark, J. J. Heyd, E. N. Brothers, K. N. Kudin, V. N. Staroverov, T. A. Keith, R. Kobayashi, J. Normand, K. Raghavachari, A. P. Rendell, J. C. Burant, S. S. Iyengar, J. Tomasi, M. Cossi, J. M. Millam, M. Klene, C. Adamo, R. Cammi, J. W. Ochterski, R. L. Martin, K. Morokuma, O. Farkas, J. B. Foresman, D. J. Fox, Gaussian, Inc., Wallingford CT, 2009.

12 M. N. Peñas-Defrutos, C. Bartolomé, M. García-Melchor and P. Espinet, *Angew. Chem., Int. Ed.*, 2019, **58**, 3501–3505.

13 (a) P. J. Hay and W. R. Wadt, *J. Chem. Phys.*, 1985, **82**, 270–283; (b) P. J. Hay and W. R. Wadt, *J. Chem. Phys.*, 1985, **82**, 299–310.

14 A. W. Ehlers, M. Böhme, S. Dapprich, A. Gobbi, A Höllwarth, V. Jonas, K. F. Köhler, R. Stegmann, A. Veldkamp and G. Frenking, *Chem. Phys. Lett.*, 1993, **208**, 111–114.

15 A. V. Marenich, C. J. Cramer and D. G. Truhlar, *J. Phys. Chem. B*, 2009, **113**, 6378–6396.